Biomedical Optics EXPRESS

Terahertz spectroscopic imaging and properties of gastrointestinal tract in a rat model

Young Bin Ji,[1] Sang-Hoon Kim,[2] Kiyoung Jeong,[3] Yuna Choi,[2] Joo-Hiuk Son,[4] Dong Woo Park,[5,6] Sam Kyu Noh,[6] Tae-In Jeon,[7] Yong-Min Huh,[2,8] Seungjoo Haam,[1,9] Sang Kil Lee,[10,11] Seung Jae Oh,[2,12] and Jin-Suck Suh[2,8,*]

[1]Yonsei Institute of Convergence Technology, Yonsei University, Seoul 120-752, South Korea
[2]YUMS-KRIBB Medical Convergence Research Institute, College of Medicine, Yonsei University, Seoul 120-752, South Korea
[3]Graduate Program for Nanomedical Science, Yonsei University, Seoul 120-749 South Korea
[4]Department of Physics, University of Seoul, Seoul 130-743, South Korea
[5]Divsion of Advanced Materials Engineering, Chonbuk National University, Jeonju 561-756, South Korea
[6]Nano Materials Evaluation Center, Korea Research Institute of Standards and Science, Daejeon 305-340, South Korea
[7]Division of Electrical and Electronics Engineering, Korea Maritime University, Busan 606-791, South Korea
[8]Department of Radiology, Severance Biomedical Science Institute, College of Medicine, Yonsei University, Seoul 120-752, South Korea
[9]Department of Chemical and Biomolecular Engineering, Yonsei University, Seoul 120-749, South Korea
[10]Department of Medicine, College of Medicine, Yonsei University, Seoul 120-752, South Korea
[11]sklee@yuhs.ac
[12]issac@yuhs.ac
[*]jss@yuhs.ac

Abstract: We have investigated basic properties of normal gastrointestinal (GI) tract tissues, including glandular stomach (GS), fore stomach (FS), large intestine (LI), small intestine (SI), and esophagus (ESO), from a rat model using terahertz (THz) reflection imaging and spectroscopy. The THz images collected from stratified squamous epithelia (SSE) of FS and ESO show a lower peak-to-peak value compared to those from columnar epithelia (CE) of GS, LI, or SI because the SSE contains less water than CE. The refractive index and absorption coefficient of FS were less than those of GS or LI, both having values similar to those of water. Additionally, we report internal reflection THz signals from ESO, although we were unable to determine the exact interface for this internal reflection.

OCIS codes: (170.6795) Terahertz imaging; (170.3880) Medical and biological imaging; (300.6495) Spectroscopy, terahertz; (170.6510) Spectroscopy, tissue diagnostics.

References and links

1. A. G. Markelz, A. Roitberg, and E. J. Heilweil, "Pulsed terahertz spectroscopy of DNA, bovine serum albumin and collagen between 0.1 and 2.0 THz," Chem. Phys. Lett. **320**(1-2), 42–48 (2000).
2. E. Pickwell, B. E. Cole, A. J. Fitzgerald, M. Pepper, and V. P. Wallace, "In vivo study of human skin using pulsed terahertz radiation," Phys. Med. Biol. **49**(9), 1595–1607 (2004).
3. B. M. Fischer, M. Hoffmann, H. Helm, R. Wilk, F. Rutz, T. Kleine-Ostmann, M. Koch, and P. U. Jepsen, "Terahertz time-domain spectroscopy and imaging of artificial RNA," Opt. Express **13**(14), 5205–5215 (2005).
4. W.-C. Kan, W.-S. Lee, W.-H. Cheung, V. P. Wallace, and E. Pickwell-Macpherson, "Terahertz pulsed imaging of knee cartilage," Biomed. Opt. Express **1**(3), 967–974 (2010).
5. S. J. Oh, J. Kang, I. Maeng, J.-S. Suh, Y.-M. Huh, S. Haam, and J.-H. Son, "Nanoparticle-enabled terahertz imaging for cancer diagnosis," Opt. Express **17**(5), 3469–3475 (2009).
6. S. J. Oh, J. Choi, I. Maeng, J. Y. Park, K. Lee, Y.-M. Huh, J.-S. Suh, S. Haam, and J.-H. Son, "Molecular imaging with terahertz waves," Opt. Express **19**(5), 4009–4016 (2011).
7. E. P. J. Parrott, S. M. Y. Sy, T. Blu, V. P. Wallace, and E. Pickwell-Macpherson, "Terahertz pulsed imaging in vivo: measurements and processing methods," J. Biomed. Opt. **16**(10), 106010 (2011).
8. L. V. Titova, A. K. Ayesheshim, A. Golubov, D. Fogen, R. Rodriguez-Juarez, F. A. Hegmann, and O. Kovalchuk, "Intense THz pulses cause H2AX phosphorylation and activate DNA damage response in human skin tissue," Biomed. Opt. Express **4**(4), 559–568 (2013).

#222459 - $15.00 USD Received 12 Sep 2014; revised 31 Oct 2014; accepted 31 Oct 2014; published 5 Nov 2014

9. S. J. Oh, S.-H. Kim, K. Jeong, Y. Park, Y.-M. Huh, J.-H. Son, and J.-S. Suh, "Measurement depth enhancement in terahertz imaging of biological tissues," Opt. Express **21**(18), 21299–21305 (2013).
10. K. Y. Jeong, Y. M. Huh, S. H. Kim, Y. Park, J. H. Son, S. J. Oh, and J. S. Suh, "Characterization of blood using terahertz waves," J. Biomed. Opt. **18**(10), 107008 (2013).
11. R. M. Woodward, V. P. Wallace, R. J. Pye, B. E. Cole, D. D. Arnone, E. H. Linfield, and M. Pepper, "Terahertz pulse imaging of ex vivo basal cell carcinoma," J. Invest. Dermatol. **120**(1), 72–78 (2003).
12. V. P. Wallace, A. J. Fitzgerald, S. Shankar, N. Flanagan, R. Pye, J. Cluff, and D. D. Arnone, "Terahertz pulsed imaging of basal cell carcinoma ex vivo and in vivo," Br. J. Dermatol. **151**(2), 424–432 (2004).
13. A. J. Fitzgerald, V. P. Wallace, M. Jimenez-Linan, L. Bobrow, R. J. Pye, A. D. Purushotham, and D. D. Arnone, "Terahertz pulsed imaging of human breast tumors," Radiology **239**(2), 533–540 (2006).
14. C. Yu, S. Fan, Y. Sun, and E. Pickwell-Macpherson, "The potential of terahertz imaging for cancer diagnosis: A review of investigations to date," Quant. Imaging Med. Surg. **2**(1), 33–45 (2012).
15. C. B. Reid, A. Fitzgerald, G. Reese, R. Goldin, P. Tekkis, P. S. O'Kelly, E. Pickwell-MacPherson, A. P. Gibson, and V. P. Wallace, "Terahertz pulsed imaging of freshly excised human colonic tissues," Phys. Med. Biol. **56**(14), 4333–4353 (2011).
16. S. J. Oh, Y.-M. Huh, S.-H. Kim, J. M. Yang, K. Y. Jeong, Y. J. Park, C. Kang, J.-H. Son, and J.-S. Suh, "Terahertz pulse imaging of fresh brain tumor," Infrared, Millimeter and Terahertz Waves (IRMMW-THz), 36th International Conference on, Houston, USA, 2–7 Oct. 2011.
17. S. J. Oh, S.-H. Kim, Y. B. Ji, K. Y. Jeong, Y. J. Park, J. Yang, D. W. Park, S. K. Noh, S. G. Kang, Y. M. Huh, J. H. Son, and J. S. Suh, "Study of freshly excised brain tissues using terahertz imaging," Biomed. Opt. Express **5**(8), 2837–2842 (2014).
18. Y. C. Sim, J. Y. Park, K.-M. Ahn, C. S. Park, and J.-H. Son, "Terahertz imaging of excised oral cancer at frozen temperature," Biomed. Opt. Express **4**(8), 1413–1421 (2013).
19. Z. D. Taylor, R. S. Singh, D. B. Bennett, P. Tewari, C. P. Kealey, N. Bajwa, M. O. Culjat, A. Stojadinovic, H. Lee, J.-P. Hubschman, E. R. Brown, and W. S. Grundfest, "THz medical imaging: In vivo hydration sensing," IEEE Trans. Terahertz Sci. Technol. **1**(1), 201–219 (2011).
20. S. Sy, S. Huang, Y.-X. J. Wang, J. Yu, A. T. Ahuja, Y.-T. Zhang, and E. Pickwell-MacPherson, "Terahertz spectroscopy of liver cirrhosis: investigating the origin of contrast," Phys. Med. Biol. **55**(24), 7587–7596 (2010).
21. E. Berry, A. J. Fitzgerald, N. N. Zinov'ev, G. C. Walker, S. Homer-Vanniasinkam, C. D. Sudworth, R. E. Miles, J. M. Chamberlain, and M. A. Smith, "Optical properties of tissue measured using terahertz pulsed imaging," Proc. SPIE: Med. Imag., **5030**, 459–470 (2003).
22. D. B. Bennett, W. Li, Z. D. Taylor, W. S. Grundfest, and E. R. Brown, "Stratified media model for terahertz reflectometry of the skin," IEEE Sens. J. **11**(5), 1253–1262 (2011).
23. E. Pickwell, A. J. Fitzgerald, B. E. Cole, P. F. Taday, R. J. Pye, T. Ha, M. Pepper, and V. P. Wallace, "Simulating the response of terahertz radiation to basal cell carcinoma using ex vivo spectroscopy measurements," J. Biomed. Opt. **10**(6), 064021 (2005).
24. S. Huang, P. C. Ashworth, K. W. C. Kan, Y. Chen, V. P. Wallace, Y.-T. Zhang, and E. Pickwell-MacPherson, "Improved sample characterization in terahertz reflection imaging and spectroscopy," Opt. Express **17**(5), 3848–3854 (2009).
25. S. Y. Huang, Y. X. J. Wang, D. K. W. Yeung, A. T. Ahuja, Y.-T. Zhang, and E. Pickwell-Macpherson, "Tissue characterization using terahertz pulsed imaging in reflection geometry," Phys. Med. Biol. **54**(1), 149–160 (2009).
26. Y. B. Ji, E. S. Lee, S.-H. Kim, J.-H. Son, and T.-I. Jeon, "A miniaturized fiber-coupled terahertz endoscope system," Opt. Express **17**(19), 17082–17087 (2009).
27. C. Rønne, L. Thrane, P.-O. Astrand, A. Wallqvist, K. V. Mikkelsen, and S. R. Keiding, "Investigation of the temperature dependence of dielectric relaxation in liquid water by THz reflection spectroscopy and molecular dynamics simulation," J. Chem. Phys. **107**(14), 5319–5331 (1997).
28. T. Sano, O. Kobori, and T. Muto, "Lymph node metastasis from early gastric cancer: endoscopic resection of tumour," Br. J. Surg. **79**(3), 241–244 (1992).

1. Introduction

Terahertz (THz) electromagnetic waves are highly sensitive to biomolecules and water content, hence they have applied to many biomedical applications [1–10]. For example, the application of THz spectroscopic imaging to cancer diagnosis has been investigated [11–18]. THz spectroscopic imaging techniques have received great attention owing to their use for cancer diagnosis in skin [11, 12] and breast tissues [13] by using differences in water content as a natural contrast agent [14]. In recent reports, researchers have shown the possibility of diagnosing other various cancers such as colonic [15], brain [16, 17], and oral cancers [18]. The fundamental principle behind diagnosing cancer with THz waves is using distinctions between THz signals reflected from normal and tumor tissues, which have different

#222459 - $15.00 USD Received 12 Sep 2014; revised 31 Oct 2014; accepted 31 Oct 2014; published 5 Nov 2014

interstitial water content [12, 13, 19] or other contrast mechanisms such as structural changes of tissue [20].

The practical direction for the application of THz techniques would be to develop an easy, quick, and accurate mean to discriminate between normal and abnormal tissue. It might reduce unnecessary excision of normal tissue during cancer surgeries as well as assisting precise localization for biopsies.

Many studies have analyzed the basic properties of biomaterials in the THz regime [21], and have addressed analysis methods for various normal tissues [7, 22–24]. Most studies were concentrated on characterization of normal skin tissues, while other organ tissue types were not studied sufficiently. For example, although GI tract consists of different tissue layers compared to skin, the basic properties of GI tract in the THz regime have been rarely reported. Because of tissue layer differences, it is conceivable that the THz waves reflected by GI tract have different aspects compared with those reflected by skin tissues. Recently, Huang et al showed THz reflection spectroscopy could be used to characterize tissues and that there were differences between the THz properties of the tissues from different organs [25]. The characterization for a few of digestive organs was reported in that study, but there has been lack of basic studies for whole GI tract in THz regime.

The purpose of this study is to show THz imaging is able to probe subtle differences between GI tract tissues using their basic tissue properties, which could potentially be useful for diagnosing (discriminating) specific types of cancer. In order to demonstrate this, we display reflection THz spectroscopic images from which we can partially distinguish each normal GI tract tissue, also, calculate the optical properties of fresh normal GI tract which can be used as control samples in cancer (or other abnormal tissue) diagnosis using THz waves. In this paper, we report the optical properties of three fresh normal GI tract tissues, including GS, FS, and LI, in the THz regime. Additionally, internal reflection THz signals from rat ESO samples are reported, and histological analysis with H & E staining photography is performed.

2. Experimental setup and sample preparation

2.1 Experimental setup

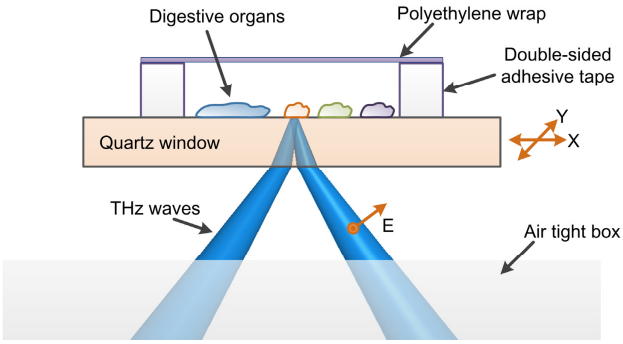

Fig. 1. Schematic diagram of the experimental setup. Five GI tract samples were placed on a quartz window and covered with polyethylene wrap to prevent dehydration.

A conventional reflection-mode THz time-domain imaging system with photoconductive antennas was utilized in our experiments. We used four off-axis parabolic reflectors to focus THz waves on samples and guide reflected waves to the detector. The focal length of used parabolic reflector was 2 inch and the F-number was 1. We didn't use any limiting aperture and the spatial resolution of our system was roughly 0.8-mm at 0.5 THz. The incident angle of THz beams focused through a quartz window was 14.6° [5, 9]. A fast optical delay line (APE) with 20 Hz operating frequency and 37 ps time window was used for fast acquisition

#222459 - $15.00 USD Received 12 Sep 2014; revised 31 Oct 2014; accepted 31 Oct 2014; published 5 Nov 2014

of THz signals. THz images were obtained with a raster scanning system using a two-dimensional (2D) movable sample stage. The acquisition time per image was approximately 26 min and 40 sec for a 50 × 40-mm area with 250-μm scanning resolution. In order to minimize influence from water vapor, THz wave paths were mostly located in an air-tight box in which humidity was less than 2%. As shown in Fig. 1, the sample stage was located outside of the air-tight box to avoid drying fresh samples by dry air during experimentation. To prevent moisture from evaporating, we attached double-sided tape around a quartz window, and then covered the samples with polyethylene tape. The temperature was kept constant during all experiments.

2.2 Sample preparation

All five fresh GI tract tissues were surgically extracted from three 35-week-old male Sprague Dawley rats after euthanasia and perfusion with saline. Samples consisted of esophagus (ESO), large intestine (LI), small intestine (SI), fore stomach (FS), and glandular stomach (GS) (rat stomach consisted of two well-defined areas: a non-glandular FS and a GS with gland separated by a limiting ridge). In order to collect measurements from the inside of samples, we split the organs and carefully removed contaminants, such as excrement, with distilled water and cotton swabs. Then, samples were carefully placed onto a 3-inch diameter and 3-mm thick quartz window without producing any air bubbles between samples and the window. All animal experiments were conducted with the approval of the Institutional Animal Care and Use Committee of Yonsei University Health System.

3. Results and discussion

The normal tissues of GI tract were partially distinguished by THz imaging. Figures 2(a) and 2(b) shows a photograph and a 2D THz image of five samples, respectively. The GS was placed in the upper left corner, and the FS was placed below the GS. The ESO, SI, and LI samples were placed in this order from the left to the right, as shown in Fig. 2(a). The THz waves were reflected at the interface between the quartz and samples, and the amplitude and phase of the reflected signals were determined by the Fresnel diffraction formula. The acquired 2D THz image was extracted using peak-to-peak values from reflected THz signals having different amplitudes and phases. Despite all samples being normal tissues, they were distinguished in the THz image. In particular, the GS and FS in Fig. 2(b) were easily distinguished. The FS produced lower peak-to-peak amplitude compared to the GS. The THz signals reflected from the biological samples may have slightly different amplitudes and phases because the tissues had slightly different local surface conditions and water content. These tissue properties resulted in the heterogeneous THz images shown in Fig. 2(b).

#222459 - $15.00 USD Received 12 Sep 2014; revised 31 Oct 2014; accepted 31 Oct 2014; published 5 Nov 2014

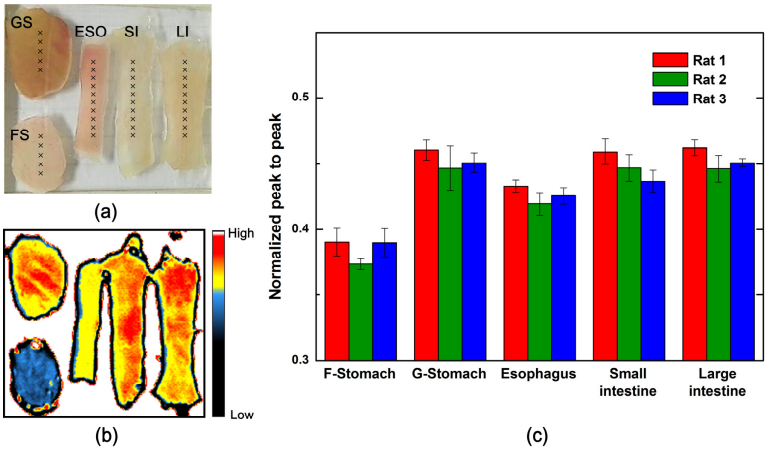

Fig. 2. (a) Optical photograph of five GI tract samples from a rat model. (b) Reflected 2D THz image with peak-to-peak values. (c) Normalized and averaged reflection peak-to-peak values for five GI tract tissues (from three different rats) analyzed at points marked in (a).

To produce reliable results, experiments were performed with three different rats. However, note that there was a limitation of small sample size (n = 3) which would undermine the reliability of our results. Normalized and averaged peak-to-peak reflected THz signal values with standard deviation obtained from the five or ten points marked in Fig. 2(a) are shown in Fig. 2(c). Our data were normalized by THz signal reflected from the interface between quartz and air to reduce other background noise. This result indicates the FS could be easily distinguished from other GI tract tissues using THz waves. The peak-to-peak amplitude of THz waves reflected from FS and ESO was smaller than those from other GI tract tissues.

In order to analyze these data, we collected reflected THz time-domain waveforms from points marked in Fig. 2(a), as well as cross-sectional H & E stained images (Fig. 3 and 5). In contrast to skin, which consists of stratum corneum, epidermis, and dermis layers, normal tissues of GI tract generally consist of mucosa, submucosa, muscle, and serosa layers. Additionally, the mucosal layer can be subdivided depending on the specific GI tract. The histological structures of samples used in this report are displayed in Table 1. These samples can be grouped simply according to components of their mucosal layers. The mucosal layers for GS, LI, and SI consist of columnar epithelium (CE), lamina propria (LP), and muscularis mucosa (MM), while mucosa of FS and ESO consist of stratified squamous epithelium (SSE), LP, and MM. These two groups are dissimilar only in their top layers of mucosa. Note that even though CE (or SSE) layers have the same histological labels, CE (or SSE) layers have slightly different shapes, thicknesses, and compositions according images shown in Fig. 3 and 5.

Table 1. Constituent layers of five GI tract tissues in a rat model

GI tract	Mucosa	Submucosa	Muscle	Serosa
GS	CE / LP / MM	O	O	O
FS	SSE / LP/ MM	O	O	O
ESO	SSE / LP/ MM	O	O	O
LI	CE / LP / MM	O	O	O
SI	CE / LP / MM	O	O	O

Figures 3(a) and 3(b) displays the measured time-domain THz signals and THz spectra reflected from water, LI, GS, and FS. The inset displays an expanded time window from 23 to 28 ps. The THz signal reflected from water, with no internal interfaces, was displayed to confirm the presence of internal reflection signals from samples. THz signals displayed in the

#222459 - $15.00 USD Received 12 Sep 2014; revised 31 Oct 2014; accepted 31 Oct 2014; published 5 Nov 2014

inset are almost same, meaning there are no reflection signals from the internal structures of these three samples. These results suggest that signals were only reflected from the interface between the quartz and CE layers of samples. We assume that the ringing signal in the figure inset is related to unwanted and unclear THz signal reflected from our experimental setup. Although the CE layers of LI and GS have different thicknesses and shapes, as shown in Figs. 3(c) and 3(d), the THz signals reflected from the analysis points of these organs are almost same. Because reflected THz signals contain amplitude and phase information about the samples, the refractive index and absorption coefficient could be calculated by referencing the THz signal reflected from the interface between quartz and metal [26].

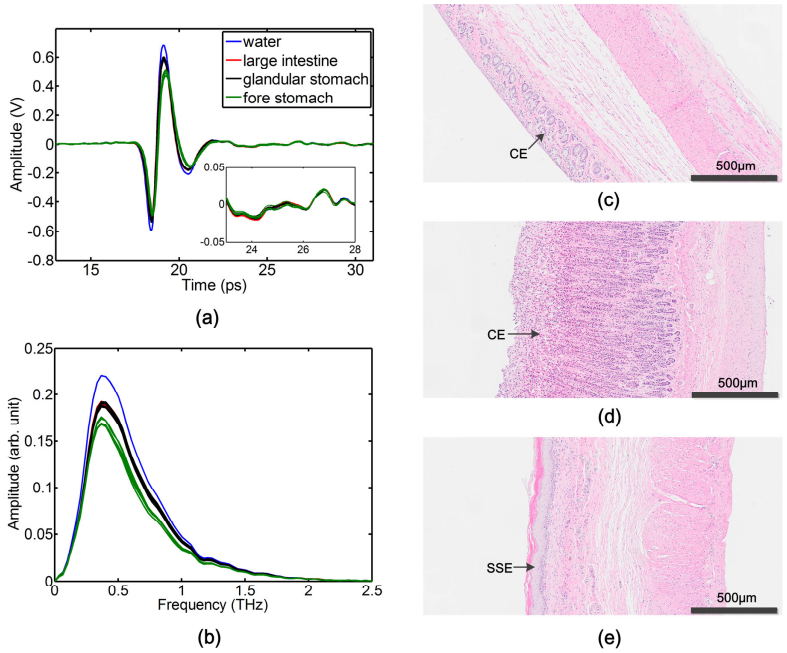

Fig. 3. (a) Measured time-domain THz signals reflected from points marked on LI, GS, FS (Fig. 2(a)), and water. Analysis of water was used to verify the presence of secondary THz signals reflected from internal interfaces within samples. The inset shows an expanded time window (23 to 28 ps). (b) Measured THz spectra of (a). (c)-(e) H & E stained photographs of LI, GS, and FS, respectively.

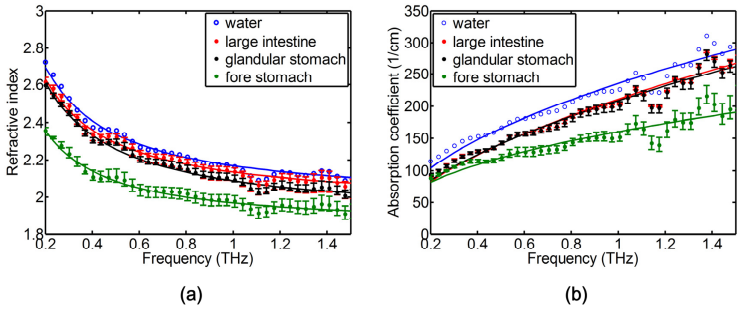

Fig. 4. (a) Measured refractive indices of water and three GI tract samples. (b) Measured absorption coefficients of water and three GI tract samples. The refractive indices and absorption coefficients of LI and GS are greater than those of FS due to a difference in water content.

The calculated refractive indices and absorption coefficients are shown in Figs. 4(a) and 4(b). To verify the accuracy of our calculations, we compared the calculated refractive index

#222459 - $15.00 USD Received 12 Sep 2014; revised 31 Oct 2014; accepted 31 Oct 2014; published 5 Nov 2014

and absorption coefficient of water with previous measurements [27]; these data were in good agreement. The refractive indices of LI and GS were 0.18 - 0.21 greater than that of FS at 0.5 THz. Additionally, the absorption coefficients of LI and GS were 22 cm^{-1} greater than that of FS at 0.5 THz. The CE layer has a high water content because it has a high cell density and is composed of glands containing digestive fluid, as shown in Figs. 3(c) and 3(d). In contrast, the SSE layer, as shown in Fig. 3(e), has no glands and fewer cells. Thus, the FS (SSE layer) has a lower refractive index and absorption coefficient than LI, GS (CE layer), or water. This result suggests that cancers occurring in the SSE layer would be easily diagnosed compared to cancers occurring in the CE layer because most cancer tissues contain more water than normal tissues [12, 13]. The large difference in refractive index and absorption coefficient values between samples in the THz regime would allow easy discrimination between cancer and normal tissues. We expect that the contrast between esophageal cancer and normal ESO tissues characterized by the SSE layer would greater than the contrast between stomach, colon, or rectum cancer and their respective normal tissues.

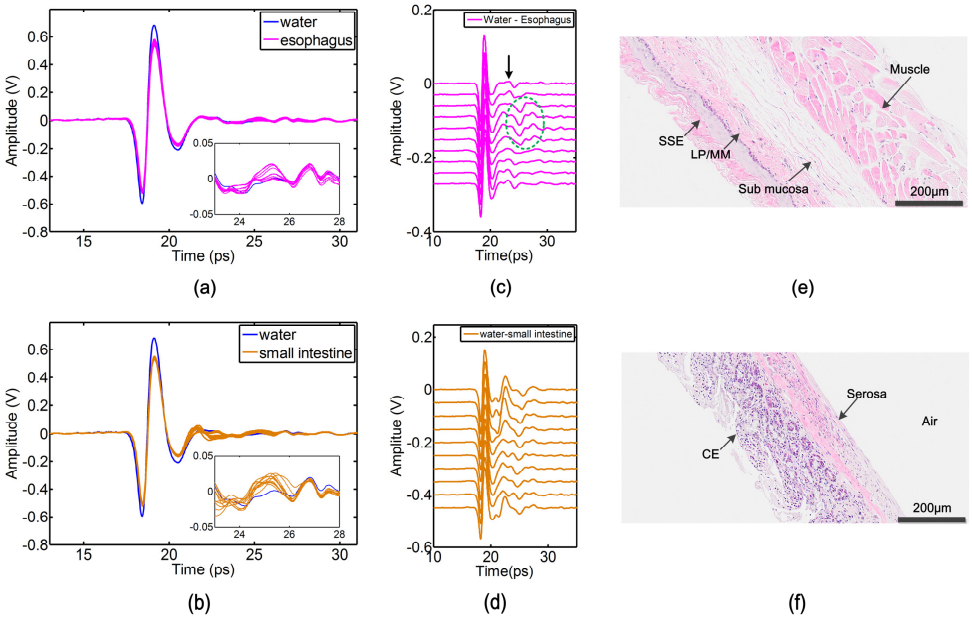

Fig. 5. (a), (b) Measured time-domain THz signals reflected from points marked on ESO and SI in Fig. 2. (c), (d) Reflection signals from ESO and SI subtracted from those of water. Black arrows indicate secondary reflection signals from internal structures within the ESO. The four secondary signals indicated with a green circle were reflected from the interface between serosa of the ESO and the air. (e), (f) H & E stained photographs of ESO and SI.

Unlike the THz signals reflected from LI, GS, and FS, the THz signals reflected from ESO and SI had secondary reflection signals, as shown in Figs. 5(a) and 5(b). The inset of Fig. 5(a) shows different characteristics when compared with the inset of Fig. 3(a). The THz signals from the ten analysis points of ESO have various shapes within the time window of 23 to 28 ps. To facilitate the observation of secondary THz signals, we subtracted the reflection signals of ESO from those of water and then displayed the numerically shifted results in Fig. 5(c). If a deconvolution [24, 25] is performed to our results the second reflections might be clearer, but we didn't acquire baseline data for deconvolution when experiments were perform, so we were not able to perfectly use the method to our results. Nevertheless, the used subtraction mean effectively reduces background noise and the subsequent second reflections were clearer, we could find presence of internal THz reflections from ESO. The positive peak positions (18.95 ps) of the large primary signals

#222459 - $15.00 USD Received 12 Sep 2014; revised 31 Oct 2014; accepted 31 Oct 2014; published 5 Nov 2014

indicate the position of THz signals reflected from the interface between quartz and the top layer of ESO. The peak positions of the small secondary signals, indicated by a black arrow in Fig. 5(c), indicate the positions of THz signals reflected from an internal structure in ESO. Note that six positions of secondary THz signals are similar, but the four secondary signals indicated with a green circle are located at delayed time positions. These four signals will be discussed later in this report. We determined the six similar secondary peak positions ranged from 23.05 to 23.42 ps. Because biological samples are dispersive materials in THz regime, and the refractive indices and absorptions of the internal layer of ESO, such as LP, MM or submucosa are not known, we assumed the refractive index of the internal layer of ESO is constant as 2.1 to calculate the thickness of the internal reflection interface. The calculated range of thicknesses of the reflection interface, using a refractive index of 2.1, was 292 - 319 μm. The total thickness of the ESO sample, measured from H & E stained photographs, was between 500 and 980 μm. Therefore, we analyzed the secondary THz signals reflected from internal structures in the ESO samples because the calculated interface thickness was much less than the total tissue thickness. The secondary signals that were reflected from internal interfaces in the ESO were confirmed with ESO tissue from other rats (data not shown). This first detection of internal THz reflections from ESO would provide a clue to determine depth of invasion which correlated closely with the lymph node metastasis in esophageal cancer or other digestive cancer [28] when THz system with very high signal to noise ratio are developed.

Figure 5(e) shows an H & E stained photograph of rat ESO, illustrating distinct interfaces between the top and inside layers, such as SSE/LP and submucosa/muscle. In order to determine which interface secondary THz signals were reflected from, we compared the calculated reflection interface thickness obtained with THz experiments with the each internal interface obtained from the H & E stained photograph. Unfortunately, no interface was an exact match. One reason for this is that the focused beam diameter of THz waves was 500 μm, but the thickness of interfaces in the ESO verified with an H & E stained photograph can be continually changing within the range of 500 μm. Additionally, though the thickness between each interface is less than 100 μm, there is the possibility of this thickness being changed by the protocol for producing H & E stained photographs, which includes formalin fixation and making paraffin blocks. A third reason for not having an exact interface match was that although we marked the measuring point on ESO samples, the marked point, measured point, and obtained point from H & E stained photographs may not have been matched.

In contrast, in the SI sample, we observe that secondary signals were not reflected from internal interfaces, but rather from the interface between serosa of the SI and air although the reflection data of the SI sample shown in Figs. 5(b) and 5(d) do not seem to significantly differ from those of the ESO sample in Figs. 5(a) and 5(c). This analysis is based on the observation of secondary signals not being reflected from SI samples over 500-μm thick. The total thickness of SI samples used was less than 300 μm, as shown in Fig. 5(f). The presence of signals reflected from interfaces between air and thin biological samples has been reported in a previous study [9]. Reflection signals from SI samples over 500-μm thick were very similar to those from LI and GS, as shown in Fig. 3(a).

Finally, we assume that the four signals indicated with a green circle in Fig. 5(c) were reflected by the interface between the serosa of ESO and air, and are similar to what was observed with thin SI. Although these signals were reflected from deeper levels (25 - 26 ps), the amplitudes were similar or greater than those of the other six secondary signals. The amplitude of signals reflected from interfaces between biological samples and air are greater than those produced by internal interfaces due to the larger difference in refractive index.

#222459 - $15.00 USD Received 12 Sep 2014; revised 31 Oct 2014; accepted 31 Oct 2014; published 5 Nov 2014

4. Summary and conclusions

We have demonstrated that THz wave analysis can distinguish between different normal GI tract tissues from a rat model. The reflected THz signal properties depend on the surface layer of each GI tract. The reflection amplitude from FS and ESO (with SSE) was lower than that from GS, LI, or SI (with CE) because the CE layer contains more water. The refractive index and absorption coefficient measurements of FS (SSE layer) were lower than those of GS and LI (CE layer), which were similar to water. This result suggests the potential for human esophageal cancers would be more easily discriminated than stomach, colon, or rectum cancer because most cancers contain a higher water content compared to normal tissues. Moreover, THz analysis would be applied to probe Barrett's esophagus, which involves a transition from SSE to CE. However, note these two statements have a bit of a hypothetical leap and there was no direct evidence. Additionally, we have reported the first internal reflection THz signals collected from ESO, though we were not able to determine the internal interface. As previously mentioned, the characterization for few of digestive organs reported in previous study [25], but there has been still lack of basic studies for whole GI tract and still lack of their basic data including refractive indices and absorption coefficients of LP, MM or submucosa. Future work will involve investigating the refractive index and absorption of LP, MM and submucosa using a pig model in which the layers are thicker than rat model and also finding the exact internal reflection interface in ESO. Additionally, we will investigate the use of THz waves for the discrimination of esophageal cancer and Barrett's esophagus. We expect this basic study to help develop a THz endoscope for the discrimination of esophageal cancer, Barrett's esophagus and other digestive organ cancers.

Acknowledgments

This study was supported by a grant from the Korean Health Technology Research and Development Project of the Ministry for Health, Welfare and Family Affairs, Republic of Korea (HI10C19110300). This work was supported in part by the Yonsei University Research Fund of 2013 and 2014.

#222459 - $15.00 USD Received 12 Sep 2014; revised 31 Oct 2014; accepted 31 Oct 2014; published 5 Nov 2014